

4.8 Gbit/s 16-QAM-OFDM transmission based on compact 450-nm laser for underwater wireless optical communication

Hassan M. Oubei,¹ Jose R. Duran,¹ Bilal Janjua,¹ Huai-Yung Wang,² Cheng-Ting Tsai,² Yu-Cheih Chi,² Tien Khee Ng,¹ Hao-Chung Kuo,³ Jr-Hau He,¹ Mohamed-Slim Alouini,¹ Gong-Ru Lin,^{2,4} and Boon S. Ooi^{1,5}

¹Computer, Electrical and Mathematical Sciences and Engineering (CEMSE) division, King Abdullah University of Science and Technology (KAUST), Thuwal 23955-6900, Kingdom of Saudi Arabia

²Graduate Institute of Photonics and Optoelectronics and Department of Electrical Engineering, National Taiwan University (NTU), Taipei 10617, Taiwan

³Department of Photonics, National ChiaoTung University (NCTU), Hsinchu 30010, Taiwan

⁴grlin@ntu.edu.tw

⁵boon.ooi@kaust.edu.sa

Abstract: We experimentally demonstrate an underwater wireless optical communications (UWOC) employing 450-nm TO-9 packaged and fiber-pigtailed laser diode (LD) directly encoded with an orthogonal frequency division multiplexed quadrature amplitude modulation (QAM-OFDM) data. A record data rate of up to 4.8 Gbit/s over 5.4-m transmission distance is achieved. By encoding the full 1.2-GHz bandwidth of the 450-nm LD with a 16-QAM-OFDM data, an error vector magnitude (EVM) of 16.5%, a signal-to-noise ratio (SNR) of 15.63 dB and a bit error rate (BER) of 2.6×10^{-3} , well pass the forward error correction (FEC) criterion, were obtained.

©2015 Optical Society of America

OCIS codes: (010.4455) Oceanic propagation; (060.2605) Free-space optical communication; (060.4510) Optical communications; (140.2020) Diode lasers; (140.7300) Visible lasers.

References and links

1. I. F. Akyildiz, D. Pompili, and T. Melodia, "Underwater acoustic sensor networks: research challenges," *Ad Hoc Netw.* **3**(3), 257–279 (2005).
2. P. Lacovara, "High-bandwidth underwater communications," *Mar. Technol. Soc. J.* **42**(1), 93–102 (2008).
3. G. Baiden, Y. Bissiri, and A. Masoti, "Paving the way for a future underwater omni-directional wireless optical communication systems," *Ocean Eng.* **36**(9–10), 633–640 (2009).
4. C. Gabriel, M. Khalighi, S. Bourennane, P. Léon, and V. Rigaud, "Monte-Carlo-based channel characterization for underwater optical communication systems," *J. Opt. Commun. Netw.* **5**(1), 1–12 (2013).
5. W. Cox and J. Muth, "Simulating channel losses in an underwater optical communication system," *J. Opt. Soc. Am. A* **31**(5), 920–934 (2014).
6. B. Cochenour, L. Mullen, and J. Muth, "Effect of scattering albedo on attenuation and polarization of light underwater," *Opt. Lett.* **35**(12), 2088–2090 (2010).
7. Y.-C. Chi, D.-H. Hsieh, C.-T. Tsai, H.-Y. Chen, H.-C. Kuo, and G.-R. Lin, "450-nm GaN laser diode enables high-speed visible light communication with 9-Gbps QAM-OFDM," *Opt. Express* **23**(10), 13051–13059 (2015).
8. D. Tsonev, H. Chun, S. Rajbhandari, J. J. D. McKendry, S. Videv, E. Gu, M. Haji, S. Watson, A. E. Kelly, G. Faulkner, M. D. Dawson, H. Haas, and D. O'Brien, "A 3-Gb/s Single-LED OFDM-Based Wireless VLC Link Using a Gallium Nitride μ LED," *IEEE Photonics Technol. Lett.* **26**(7), 637–640 (2014).
9. S. Arnon, "Underwater optical wireless communication network," *Opt. Eng.* **49**(1), 015001 (2010).
10. A. Munafo, E. Simetti, A. Turetta, A. Caiti, and G. Casalino, "Autonomous underwater vehicle teams for adaptive ocean sampling: a data-driven approach," *Ocean Dyn.* **61**(11), 1981–1994 (2011).
11. B. Cochenour, L. J. Mullen, and A. E. Laux, "Characterization of the beam-spread function for underwater wireless optical communications links," *J. Oceanic Eng.* **33**(4), 513–521 (2008).
12. S. Tang, Y. Dong, and X. Zhang, "Impulse response modeling for underwater wireless optical communication links," *IEEE Trans. Commun.* **62**(1), 226–234 (2014).
13. F. Hanson and S. Radic, "High bandwidth underwater optical communication," *Appl. Opt.* **47**(2), 277–283 (2008).

14. S. Watson, M. Tan, S. P. Najda, P. Perlin, M. Leszczynski, G. Targowski, S. Grzanka, and A. E. Kelly, "Visible light communications using a directly modulated 422 nm GaN laser diode," *Opt. Lett.* **38**(19), 3792–3794 (2013).
 15. H. M. Oubei, C. Li, K.-H. Park, T. K. Ng, M.-S. Alouini, and B. S. Ooi, "2.3 Gbit/s underwater wireless optical communications using directly modulated 520 nm laser diode," *Opt. Express* **23**(16), 20743–20748 (2015).
 16. K. Nakamura, I. Mizukoshi, and M. Hanawa, "Optical wireless transmission of 405 nm, 1.45 Gbit/s optical IM/DD-OFDM signals through a 4.8 m underwater channel," *Opt. Express* **23**(2), 1558–1566 (2015).
 17. W. Shieh and I. Djordjevic, *OFDM for Optical Communications* (Academic Press, 2009), Chap. 2.
 18. Y. M. Lin and P. L. Tien, "Next-generation OFDMA-based passive optical network architecture supporting radio-over-fiber," *IEEE J. Sel. Top. Area Commun.* **28**(6), 791–799 (2010).
 19. J. W. Giles and I. N. Bankman, "Underwater optical communications systems. Part 2: basic design considerations," in *Proceedings of IEEE Military Communications Conf., Vol. 3* (MILCOM, 2005), pp. 1700–1705.
 20. N. G. Jerlov, *Marine Optics* (Elsevier Science, 1976).
-

1. Introduction

Human activities in underwater such as oceanography studies, offshore oil exploration, sea floor survey and monitoring have significantly increased. As a result, there is a growing need for reliable and high data-rate underwater wireless communication (UWOC) systems. Traditionally, acoustic waves have been used to establish underwater communication. However, the bandwidth of underwater acoustic channel is limited to hundreds of kHz because of strong frequency dependent attenuation of sound in seawater [1]. The slow propagation of sound waves causes large time delay in acoustic communication systems. In addition, radio frequency (RF) communication is severely limited due to the conductivity of seawater at radio frequencies [2]. Recently, the UWOC system has gained a renewed interest from military and academic research communities and has been proposed as an alternative or complementary solution to acoustic and RF underwater communication links over short and moderate distances (< 100m) [3–6]. This is due to the wide technological advances in visible light emitters, receivers, digital communications and signal processing [7, 8]. By exploiting the low absorption of seawater in blue-green (400–550 nm) region of the visible light window of electromagnetic spectrum, the UWOC system is expected to provide high data-rates to transmit large data capacity for versatile applications such as underwater oil pipe inspection, remotely operated vehicle (ROV) and sensor networks [9, 10].

The underwater propagation of light is governed by attenuation which is a combined effect of absorption and scattering mechanisms. Because of the aquatic environment is optically very challenging [11], the effect of multiple scattering especially in turbid littoral waters strongly degrades bit error rate (BER) performance of the on-off keying (OOK) based high data-rate UWOC systems [12]. Hanson *et al.* used an externally modulated laser at 1064 nm, and is frequency doubled to 532 nm in a periodically poled lithium niobate (PPLN) crystal to establish 1 Gbit/s OOK link in a 2-m water tank [13]. Although systems using conventional serial modulations such as non-return-to-zero (NRZ) OOK are cost-effective, it is difficult to increase the transmission capacity. The limited bandwidth (~1.5 GHz) of currently available gallium nitride (GaN) based visible lasers [14] puts an upper bound on the data rate and becomes very difficult to push the data rate beyond 2.3 Gbit/s [15]. To achieve higher data rates and maximize the transmission capacity of the system, spectrally efficient modulation techniques have to be exploited. Very recently, a 1.45 Gbit/s QAM-OFDM data transmission over 4.8-m underwater link has been demonstrated [16] using a 405-nm LD.

In this paper, we experimentally demonstrate an underwater wireless optical transmission at 4.8 Gbit/s over 5.4-m link using high-spectral efficient 16-QAM-OFDM modulation scheme. Our communication system uses a 450-nm fiber-pigtailed blue laser diode as optical transmitter and an avalanche photodiode (APD) module as receiver. During experiments, the constellation plot, error vector magnitude (EVM), signal-to-noise ratio (SNR) and BER are measured for the carried 16-QAM-OFDM data.

2. Experimental setup

Figure 1 depicts the measurement setup of the 16-QAM-OFDM transmission over underwater channel. The transmitter is a low cost, commercially available, TO-9 packaged and single-mode fiber-pigtailed LD (Thorlabs LP450-SF15) with an emitting wavelength of 449 nm and an output power of 15 mW biasing at 137 mA.

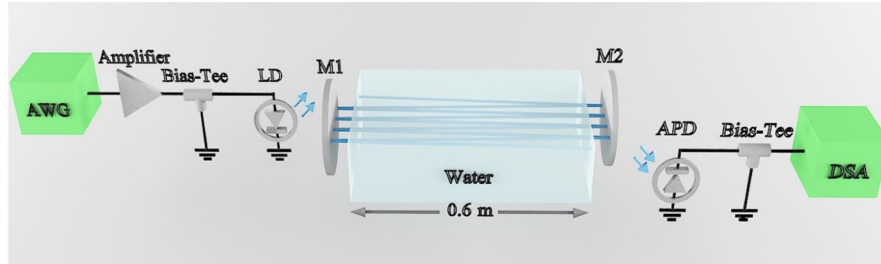


Fig. 1. Experimental setup of QAM-OFDM data transmission over 5.4-m underwater wireless optical channel: arbitrary waveform generator (AWG), laser diode (LD), mirror (M1, M2), avalanche photodiode (APD), digital serial analyzer (DSA).

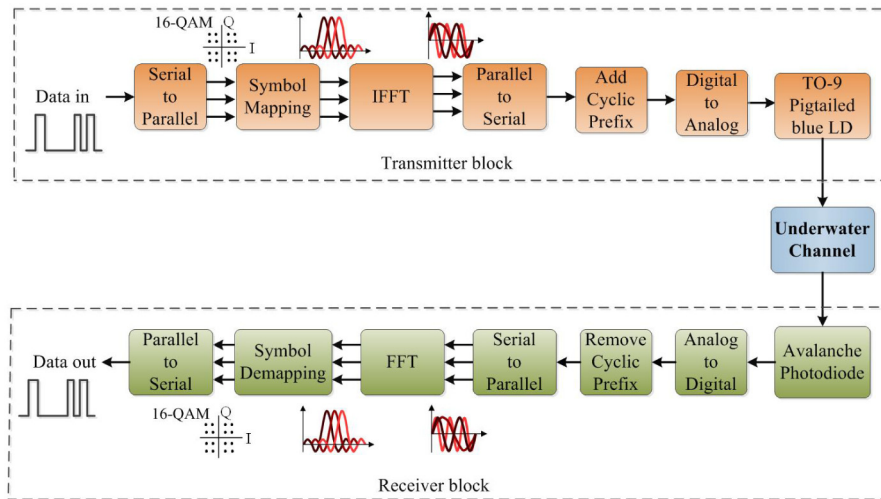


Fig. 2. Conceptual block diagram for underwater 16-QAM-OFDM transmission.

The 16-QAM-OFDM signals with corresponding subcarriers are generated by an offline Matlab[®] program and sampled by an arbitrary waveform generator (Tektronix, 70001A) with a sampling rate of 24 GSa/s. The conceptual block diagram of the 16-QAM-OFDM data generation and underwater transmission is illustrated in Fig. 2. First, a binary bit sequence is divided into parallel low-speed data blocks and mapped into QAM symbols. Details on serial-to-parallel data mapping and encoding procedure can be found in references [17, 18]. The inverse fast Fourier transform (IFFT) module converts the QAM symbols into temporal OFDM signals with a FFT size of 512. A cyclic prefix (CP) of 1/32 is added to mitigate inter-symbol interference (ISI) in the transmission link. Table 1 summarizes the related parameters of the 16-QAM-OFDM data streams to be delivered by the TO-9 packaged blue LD, including symbol length, subcarrier frequency and subcarrier frequency interval under different transmitted data rates.

Table 1. The related parameters of the 16-QAM-OFDM data stream.

Symbol Length	Subcarrier Frequency Interval	Subcarrier Frequency Range	Data Bandwidth	Data Rate (Gbit/s)
21.33 ns	46.875 MHz	0.14 to 0.54 GHz	0.4 GHz	1.6
		0.14 to 0.74 GHz	0.6 GHz	2.4
		0.14 to 0.94 GHz	0.8 GHz	3.2
		0.14 to 1.14 GHz	1.0 GHz	4
		0.14 to 1.24 GHz	1.1 GHz	4.4
		0.14 to 1.34 GHz	1.2 GHz	4.8
		0.14 to 1.44 GHz	1.3 GHz	5.2

After digital-to-analog conversion (DAC), the QAM-OFDM signals are electrically pre-amplified with a 26-dB broadband amplifier (Picosecond Pulse Labs, 5865) and then superimposed on the DC bias current using the RF connector of the built-in Bias-tee within the diode mount (Thorlabs LDM9LP), which directly encodes the TO-9 packaged blue LD. The DC bias point of the TO-9 packaged blue LD must be optimized for achieving largest peak-to-average power ratio (PAPR) of the modulated QAM-OFDM data stream. Electrical-to-optical domain conversion is performed according to the power-to-current response of the blue LD, leading to the optical 16-QAM-OFDM data stream with its maximal/minimal power levels ($P_{out,max}/P_{out,min}$) decided by the maximal/minimal ($I_{out,max}/I_{out,min}$) current levels. Figure 3 illustrates the operation of the 16-QAM-OFDM data which directly encoded onto the TO-9 packaged blue LD after offsetting by a DC bias current.

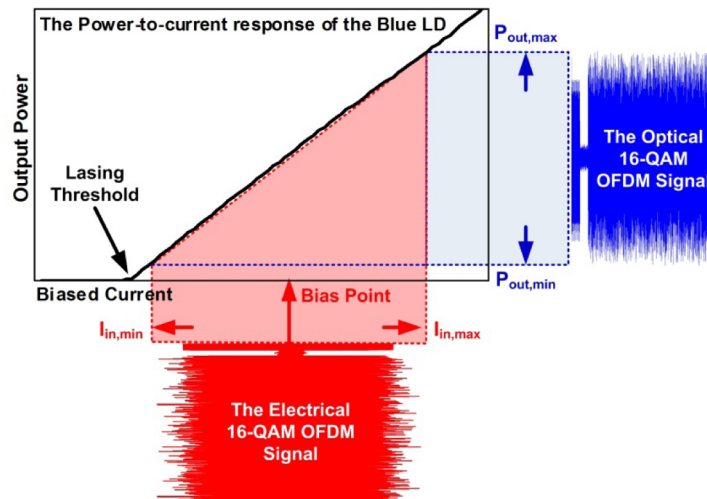


Fig. 3. The schematic diagram of the DC offset 16-QAM-OFDM data directly encoded onto the TO-9 packaged blue LD.

Afterwards, a plano-convex lens (Thorlabs LA1951-A) with 25.4-mm diameter and 25.4-mm focal length is used in front of the blue LD to produce a parallel free-space beam. The collimated laser beam with an estimated divergence angle of 5.6° is then transmitted through a water tank filled with fresh tap water with an estimated attenuation coefficient of 0.071 m^{-1} [19], similar to a clear ocean water type. The 15 mW (11.8 dBm) output power of the LD is sufficient to overcome the attenuation in clear ocean waters. The water tank with $0.6\text{-m} \times 0.3\text{-m}$ dimensions is made of glass. The physical light propagation distance was extended up to 5.4-m by using reflective mirrors installed at both ends of the tank. With using a 50-mm focal length lens, the output signal from the water channel was focused into a high sensitivity, 1-GHz bandwidth silicon APD (Menlo Systems APD210) receiver with an active diameter of

0.5-mm, a responsivity of around 5 A/W at 450 nm and a noise equivalent power (NEP) of 0.4 pW/Hz^{1/2}. The power level of transmitted laser light was controlled via neutral density filters.

After optical-electrical conversion, the received analog waveform is captured by a digital serial analyzer (Tektronix, DSA71604C) with a sampling rate of 100 GSa/s and converted to digital signals. After the removal of CP, the received OFDM signals are sent into the FFT module, which converts to frequency-domain subcarriers and re-maps back to QAM symbols. Finally, a parallel-to-serial module is employed to convert the QAM symbols into serial on-off keying data. Constellation diagram, error vector magnitude (EVM), signal-to-noise ratio (SNR) and bit error rate (BER) are measured and used to evaluate the performance of this underwater wireless optical communication system. All measurements were taken under normal room illumination and no optical interference filter was used to suppress the ambient light.

3. Results and discussion

The light-current-voltage (LIV) characteristics of the TO-9 packaged and fiber-pigtailed blue LD used in this study is shown in Fig. 4(a). The threshold current and differential quantum efficiency is 34 mA and 0.27 W/A, respectively. In Fig. 4(b), we show the lasing spectra versus wavelength at 25°C under different bias currents, which is measured by using an Ocean Optics HR4000 Spectrometer. The nominal spectral width of blue LD is 0.9 nm. The peak emitting wavelength is observed around 448.4 nm for the blue LD biased at 40 mA and is slightly red-shifted with increasing the bias current. It is worth noting that, the 448 nm blue LD is more suitable for low-loss transmission in clear ocean water types. However, the optimum wavelength of operation in an underwater optical link depends on the water turbidity which varies widely between geographic locations as defined by Jerlov water types [20]. As we go from clear ocean water types to coastal and harbor waters closer to land, the concentration of particulates (organic and inorganic) in the water is much higher, and as a result the wavelength of maximum transmission is shifted from blue wavelengths to green.

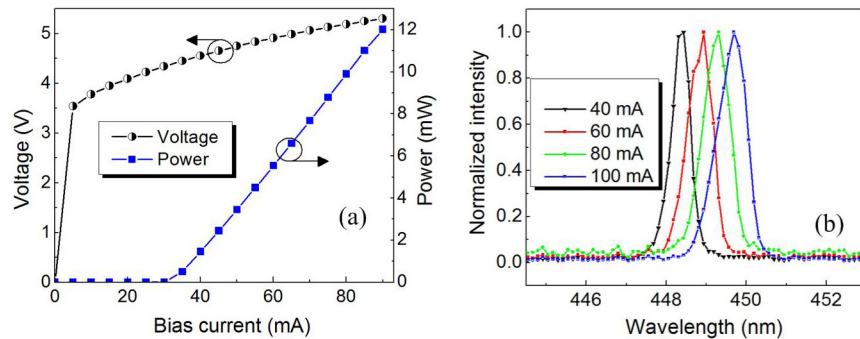


Fig. 4. (a) LIV characteristics of the blue LD at 25°C and (b) optical spectrum of the blue LD at 25°C with increasing bias current.

As a figure of merit, the overall frequency response of the system which includes the laser driver, the LD, the underwater channel, and the APD is characterized to determine the maximum allowable modulation bandwidth for encoding the OFDM signals. Figure 5 represents the small-signal modulation response at different bias currents of the blue LD, which was measured by using a vector network analyzer. When the bias current is increased, no significant extension in LD modulation bandwidth is observed due to the combined bandwidth limitations of the LD driver and the 1-GHz cut-off frequency of the APD. The decreased throughput intensity at high frequency region is also due to these bandwidth constraints. As a result, these limitations set an upper limitation on the allowable OFDM

bandwidth. The maximum -3 dB bandwidth occurs around 1.1 GHz, as indicated by the dash line in the figure.

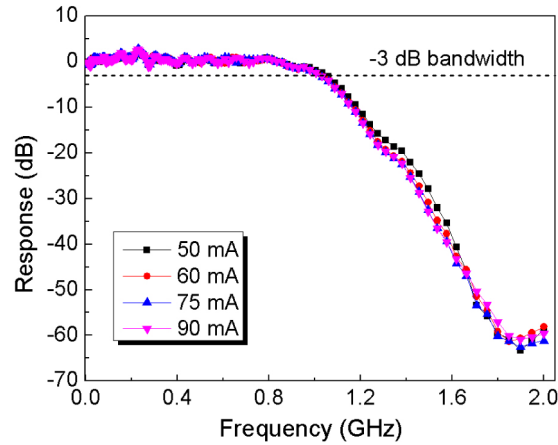


Fig. 5. Overall frequency response of the system at different LD bias currents. The dash line shows that the -3 dB bandwidth is approximately 1.1 GHz.

Before underwater transmission, the directly modulated performance of the blue LD with 1-GHz 16-QAM-OFDM data at different bias currents was firstly investigated in free-space. Both the laser bias current and the amplitude of modulating signal need to be adjusted to investigate the optimized operating condition. At low bias operation, the clipping of modulating signal degrades the BER of encoded 16-QAM-OFDM data. In addition, overly driving the blue LD declines the throughput response and ultimately degrades the high-frequency subcarrier power of the 16-QAM-OFDM data, resulting in an increased transmitted BER. The highest data rate was achieved when the bias current of blue LD and the peak-to-peak voltage of modulating signal was set to $V_{bias} = 5.01$ V ($I_{bias} = 70$ mA) and $V_{pp} = 0.4$ V, respectively. Figure 6 shows the BER performance of the blue LD delivered 1-GHz 16-QAM-OFDM data as a function of laser bias current and the constellation diagram at 70 mA.

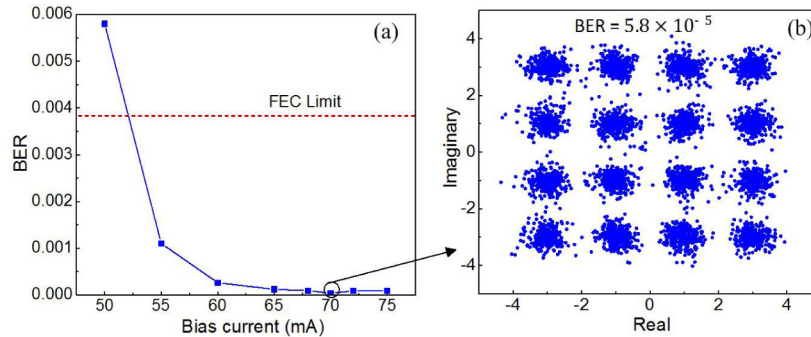


Fig. 6. Transmission performance of the blue LD carried 1 GHz 16-QAM OFDM data: (a) measured BER versus laser bias current, (b) constellation diagram at 70 mA.

To implement the underwater 16-QAM-OFDM transmission, the bias current of the blue LD was kept at the optimized operating condition of 70 mA. To evaluate the overall 16-QAM-OFDM transmission performance over the 5.4-m underwater communication channel, the measured BER, SNR and constellation plot are shown in Fig. 7. Figure 7(a) illustrates the measured BER of the 16-QAM-OFDM data versus modulation bandwidth. As a result, increasing the data bandwidth from 0.8 to 1.2 GHz enlarges the transmission capacity of the

TO-9 packaged and fiber-pigtailed blue LD from 3.2 Gbit/s to 4.8 Gbit/s at the expense of degraded BER from 6.8×10^{-4} to 2.6×10^{-3} . Further increasing the data bandwidth to 1.3 GHz leads to an increased BER of 4.8×10^{-3} , which is slightly above the FEC required BER of 3.8×10^{-3} . Therefore, to meet the FEC criterion, the acceptable bandwidth for the carried 16-QAM-OFDM is 1.2 GHz and the corresponding data rate is 4.8 Gbit/s. In Fig. 7(b), we present the measured electrical SNRs of the received 16-QAM-OFDM data as a function of subcarrier index. The measured SNR profile exhibits a negative slope and follows the overall frequency response depicted in Fig. 5. The SNR maintains high values at small subcarrier indices (low frequencies) and is inversely proportional to the subcarrier index. The average SNR at 70 mA is around 15.6 dB, which is higher than that of 15.19 dB required by the FEC decoding. Figure 7(c) shows the constellation map of 1.2-GHz 16-QAM-OFDM signals transmitted over the 5.4-m underwater channel. As shown in the figure, a clear constellation diagram can be obtained.

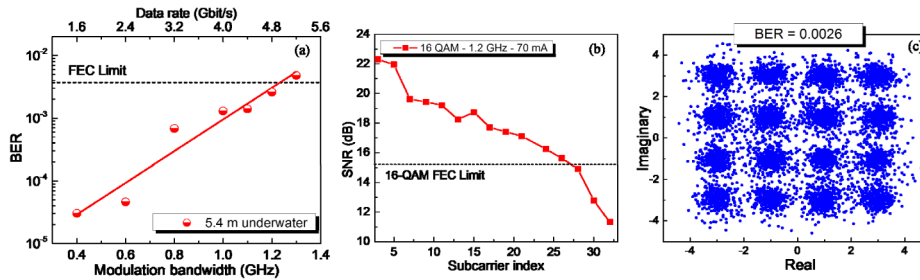


Fig. 7. Transmission performance of the blue LD delivered 16-QAM-OFDM data over 5.4-m water link: (a) Raw data rate and related BER, (b) SNR versus subcarrier index, and (c) Constellation diagram of 1.2 GHz 16-QAM-OFDM signals.

Finally, we investigate the scattering effects such as the temporal pulse spread (inter-symbol interference) on the system performance. Figure 8 shows the measured BER versus link distance for the 1.2-GHz 16-QAM-OFDM signals. The aim of this figure is to evaluate if the BER performance deteriorates as a function of link distance. It should be noted that the receiving optical power was kept constant by using a variable attenuator as the link distance was increased from 0.6 to 5.4 m. As shown in the figure, a relatively flat BER is observed. Note that the BER performance may be degraded when overly increasing the transmission distance or changing the water medium to more turbid littoral waters. This UWOC system requires good pointing accuracy between the transmitter and receiver because the transmitter beam is collimated with a very small diameter. Expanding the transmitter beam to reduce the pointing accuracy requirement will result in a weaker beam at the receiver that will reduce the performance at longer ranges. In more turbid waters, scattering increases because of high concentration of organic and inorganic particulates and can cause significant temporal dispersion which can be thought of as a form of inter-symbol interference that will reduce the pointing accuracy because the beam will spread out leading to low SNR and poor BER. However, our experimental results show that the scattering has no effect on BER performance of 1.2-GHz 16-QAM-OFDM signals during 5.4-m clear water communication link. For 4.8 Gbit/s UWOC, both the measured EVM of 16.5% and BER of 2.6×10^{-3} pass the FEC criterion, and our transmission capacity is more than three times of that reported in [16].

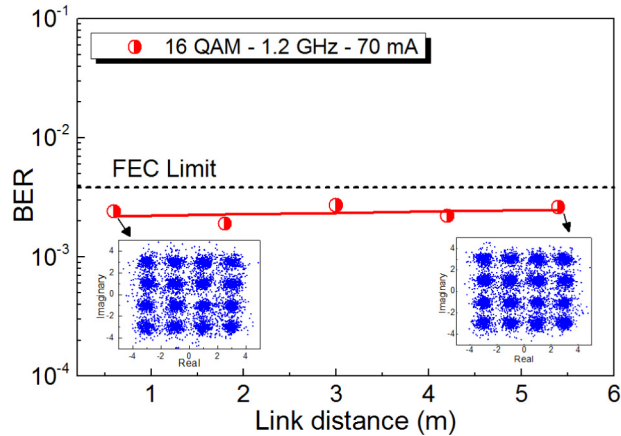


Fig. 8. Measured BER versus link distance for the 1.2-GHz 16-QAM-OFDM data with corresponding constellation diagrams at 0.6 m and 5.4 m.

4. Conclusion

In this paper, we have experimentally realized a 16-QAM-OFDM based underwater wireless optical communications system employing the 450-nm blue LD. A record data rate of up to 4.8 Gbit/s over 5.4-m transmission distance is achieved after utilizing the full 1.2-GHz bandwidth of the TO-9 packaged and fiber-pigtailed blue LD. The measured EVM and SNR of the transmitted 16-QAM-OFDM data are 16.5% and 15.63 dB, respectively. The corresponding BER is 2.6×10^{-3} , which is below the FEC required 3.8×10^{-3} . In addition, experimental results reveal that the scattering has no effect on BER performance of the transmitted 1.2-GHz 16-QAM-OFDM signals for a link distance of up to 5.4-m in clear water. Therefore, longer underwater transmission is possible by simply increasing the transmission distance since the attenuation coefficient of the water is very small. Future studies will examine the BER performance of UWOC systems at longer ranges as a function of data rate and water turbidity. This study shows that QAM-OFDM proves to be an effective solution for robust and reliable LDs based high data-rate next-generation UWOC systems.

Acknowledgment

This work was performed in National Taiwan University (NTU). Hassan Makine Oubei gratefully acknowledges the financial support from King Abdullah University of Science and Technology (KAUST), under KAUST baseline funding; KAUST Competitive Center Funding (Red Sea Research Center), and KACST TIC (Technology Innovation Center) for Solid State Lighting at KAUST.